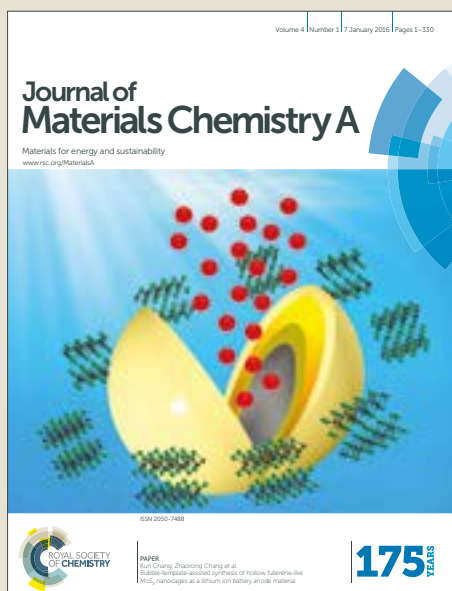


Journal of Materials Chemistry A

Accepted Manuscript



This article can be cited before page numbers have been issued, to do this please use: X. Ding, C. Chen, L. Sun, H. Li, H. Chen, J. Su, H. Li, H. Li, L. Xu and M. Cheng, *J. Mater. Chem. A*, 2019, DOI: 10.1039/C9TA00654K.



This is an Accepted Manuscript, which has been through the Royal Society of Chemistry peer review process and has been accepted for publication.

Accepted Manuscripts are published online shortly after acceptance, before technical editing, formatting and proof reading. Using this free service, authors can make their results available to the community, in citable form, before we publish the edited article. We will replace this Accepted Manuscript with the edited and formatted Advance Article as soon as it is available.

You can find more information about Accepted Manuscripts in the [author guidelines](#).

Please note that technical editing may introduce minor changes to the text and/or graphics, which may alter content. The journal's standard [Terms & Conditions](#) and the ethical guidelines, outlined in our [author and reviewer resource centre](#), still apply. In no event shall the Royal Society of Chemistry be held responsible for any errors or omissions in this Accepted Manuscript or any consequences arising from the use of any information it contains.

Highly Efficient Phenothiazine 5, 5-Dioxide-Based Hole Transport Materials for Planar Perovskite Solar Cells with PCE Exceeding 20%

Xingdong Ding,^a Cheng Chen,^{a*} Linghao Sun,^a Hongping Li,^a Hong Chen,^c Jie Su,^d Huaming Li,^{a*} Henan Li,^b Li Xu,^a Ming Cheng,^{a*}

^a Institute for Energy Research, Key Laboratory of Zhenjiang, Jiangsu University, Zhenjiang 212013, PR China

* E-mail: chencheng@ujs.edu.cn, lihm@ujs.edu.cn, mingcheng@ujs.edu.cn.

^b School of Chemistry and Chemical Engineering, Jiangsu University, Zhenjiang 212013, P. R. China

^c School of Environmental Science and Engineering, Southern University of Science and Technology, Shenzhen 518055, P. R. China

^d College of Chemistry and Molecular Engineering, Peking University, Beijing 100871, P. R. China

Keywords: planar structure, perovskite solar cell, no hysteresis, hole transport material, phenothiazine 5, 5-dioxide,

Abstract

Two novel phenothiazine 5,5-dioxide (PDO) core building block-based hole transport materials (HTMs), termed PDO1 and PDO2, were designed and synthesized. The introduction of sulfonyl group on core unit can deeply influence the energy levels and charge carrier mobilities of relative HTMs. The combined suitable energy level alignment, higher hole mobility and conductivity, as well as highly-efficient hole transfer for PDO2 make the perovskite solar cell (PSC) reach an impressive power conversion efficiency (PCE) of 20.2% and good stability when aged in ambient condition. These results demonstrate the potential versatility of the PDO building block for further development of cost-effective and highly-efficient HTMs for PSCs.

In the past few years, the power conversion efficiencies (PCEs) of PSCs have been rapidly boosted from the initial 3.8% in 2009 to over 23%.^{1,2} Such a large increase in PCEs is inseparable from the excellent hole transport property and the effective suppression of charge recombination of hole transport material (HTM) in PSCs. At present, the most commonly used HTMs are 2,2',7,7'-Tetrakis-(*N,N*-di-4-methoxyphenylamino)-9,9'-spiro bifluorene (Spiro-OMeTAD) and poly (triarylamine) (PTAA).³⁻⁵ However, because of the complicated synthetic routes of the Spiro-OMeTAD and PTAA, their synthetic costs are prohibitively high, limiting their large-scale application in future commercialization.^{6,7} Therefore, it is highly appreciated to develop or search for low-cost and highly efficient alternatives to Spiro-OMeTAD and PTAA, aiming at reaching state-of-the-art photovoltaic performance.⁸⁻²⁹ Phenothiazine 5,5-dioxide (PDO) is a heterocyclic conjugated unit, which can be easily obtained by one step oxidation from phenothiazine (PTZ) (6\$/kg). The 3-, 7- and *N*- position of PDO monomer can be easily tailored, providing easy access to a wide library of HTMs. Oxidizing PTZ to PDO would also have significant impacts on molecular conformation, which will in turn affect HTM stacking behavior in film state and charge carrier transport properties. Furthermore, the conversion of electron-donating sulfur atom to electron-withdrawing sulfone group would change the charge affinity of the core unit. To the best of our knowledge, the HTM incorporating PDO core unit has not been reported. The possible impacts of sulfone group on charge carrier transport property and photovoltaic performance are very intriguing to us and thus motivated our studies.

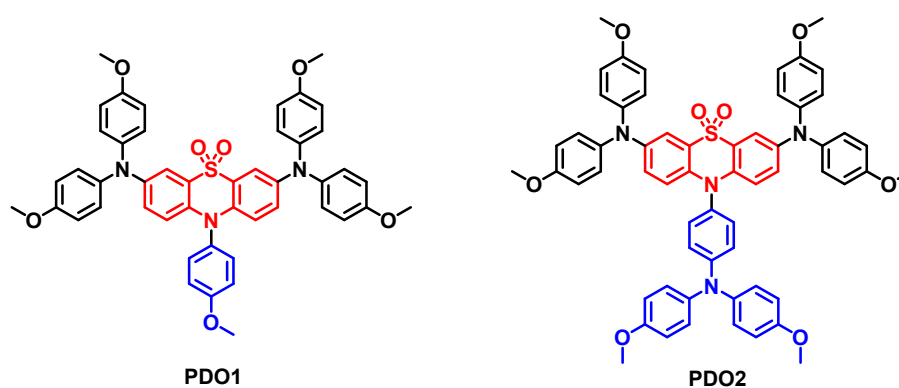


Figure 1 Molecular structures of HTMs PDO1 and PDO2

Based on these concerns, herein, we report two facilely synthesized PDO core building block based HTMs (see Figure 1). PDO has a symmetrical nonplanar structure. By substituting its 3- and 7-positions with 4,4'-dimethoxydiphenylamine, and substituting the *N*-position with anisole or 4,4'-dimethoxytriphenylamine as the peripheral groups afforded HTMs PDO1 and PDO2, respectively. With the conversion of electron-donating sulfur atom to electron-withdrawing sulfone group (from PTZ to PDO), the charge affinity of core unit is increased, making the designed HTMs PDO1 and PDO2 possess a donor-acceptor-donor (D-A-D) structure. According to molecular orbital hybridization theory, the formation of D-A-D structure can rationally decrease the highest occupied molecular orbital (HOMO) energy level and improve the intrinsic charge carrier transport properties.^{30, 31} The introduction of two 4,4'-dimethoxydiphenylamine groups on PDO unit are supposed to further adjust the energy level and charge carrier mobility, while the *N*-substitutions are to tune the spatial configuration of HTMs. The specific impact of sulfone group and different *N*-substituent groups on the material properties and photovoltaic performance were systematically studied. These two PDO-based HTMs show high hole mobility, high conductivity and suitable HOMO and lowest unoccupied molecular orbital (LUMO) levels. Through optimization, the PSCs employing PDO2 as HTM show PCEs up to 20.2%, and good stability when aged in ambient condition in the dark for 500 h. PDO1 and PDO2 were facilely synthesized through four steps, involving Buchwald-Hartwig reaction, radical substitution, and oxidation reaction. The detailed synthetic routes for PDO1 and PDO2 are depicted in Supporting Information. The synthetic costs of PDO1 and PDO2 are calculated to be 62.1791\$/g and 61.2761\$/g, respectively, which are much lower than that of Spiro-OMeTAD.^{6, 7} The synthesized HTMs were fully characterized by nuclear magnetic resonance (NMR), high-resolution mass spectrum (HRMS) and single crystal X-ray diffraction technologies.

From the crystal structures of PDO1 and PDO2, significant geometry difference can be observed on the configuration of PDO core unit in PDO1 and PDO2. The PDO unit in PDO1 is a twisted butterfly configuration, while it becomes more planar in PDO2 (see Figure 2a and Figure S7). PDO1 crystallizes in the monoclinic space group of *C2/c* with

four crystallographic independent molecules in the unit cell. The PDO1 molecules form alternately zig-zag chain along the crystallographic c axis through π - π stacking interaction (see Figure 2b). In contrast, PDO2 crystallizes in the monoclinic space group $I2/a$. As shown in Figure 2d, different than PDO1, because of the more planar configuration of PDO core unit in PDO2, the two adjacent molecules are tightly packed together related with a mirror operation or inversion center because of the strong steric-hinrance effect of N -substitution. The tight packing behavior is beneficial for intermolecular hole hopping. For both PDO1 and PDO2, each molecule has multiple short contacts distance with adjacent molecules from the same and surrounding unit cells including CH/ π hydrogen bonds and oxygen-carbon contacts, providing path for hole hopping.

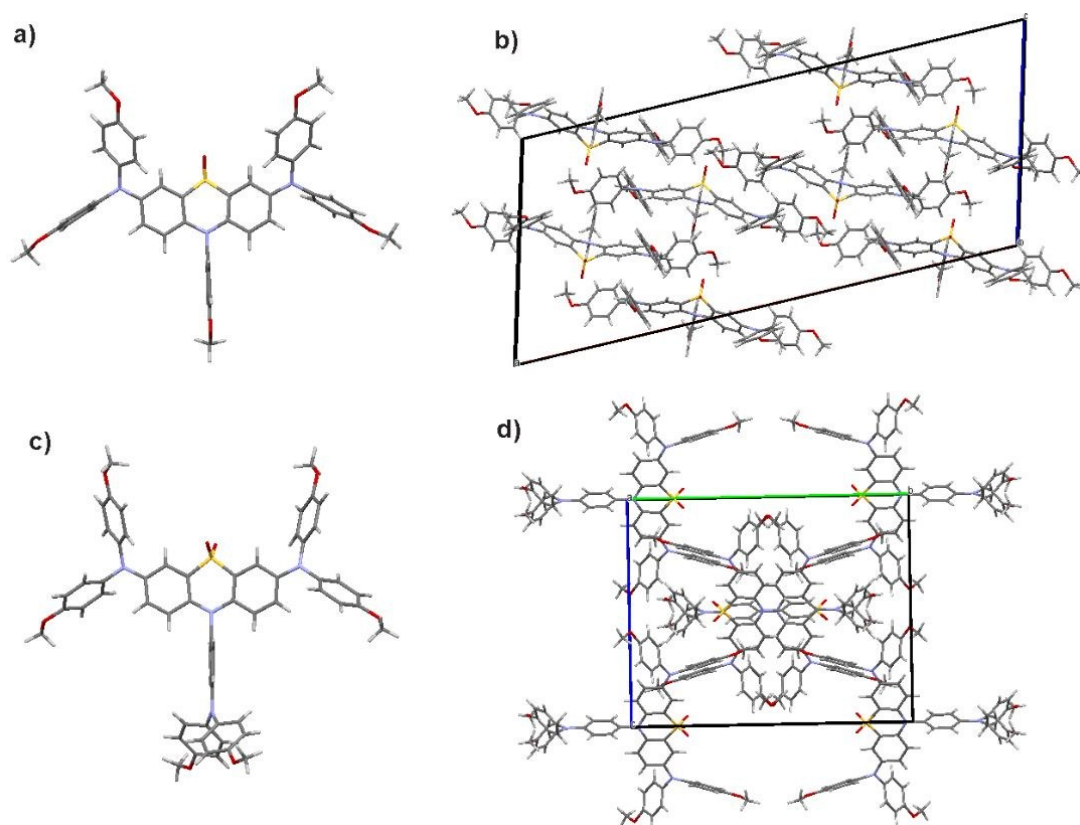


Figure 2 a) Crystal structure of HTM PDO1, b) Molecular stacking of PDO1 view along the b axis, c) Crystal structure of HTM PDO2 and d) Molecular stacking of PDO2 along the a axis.

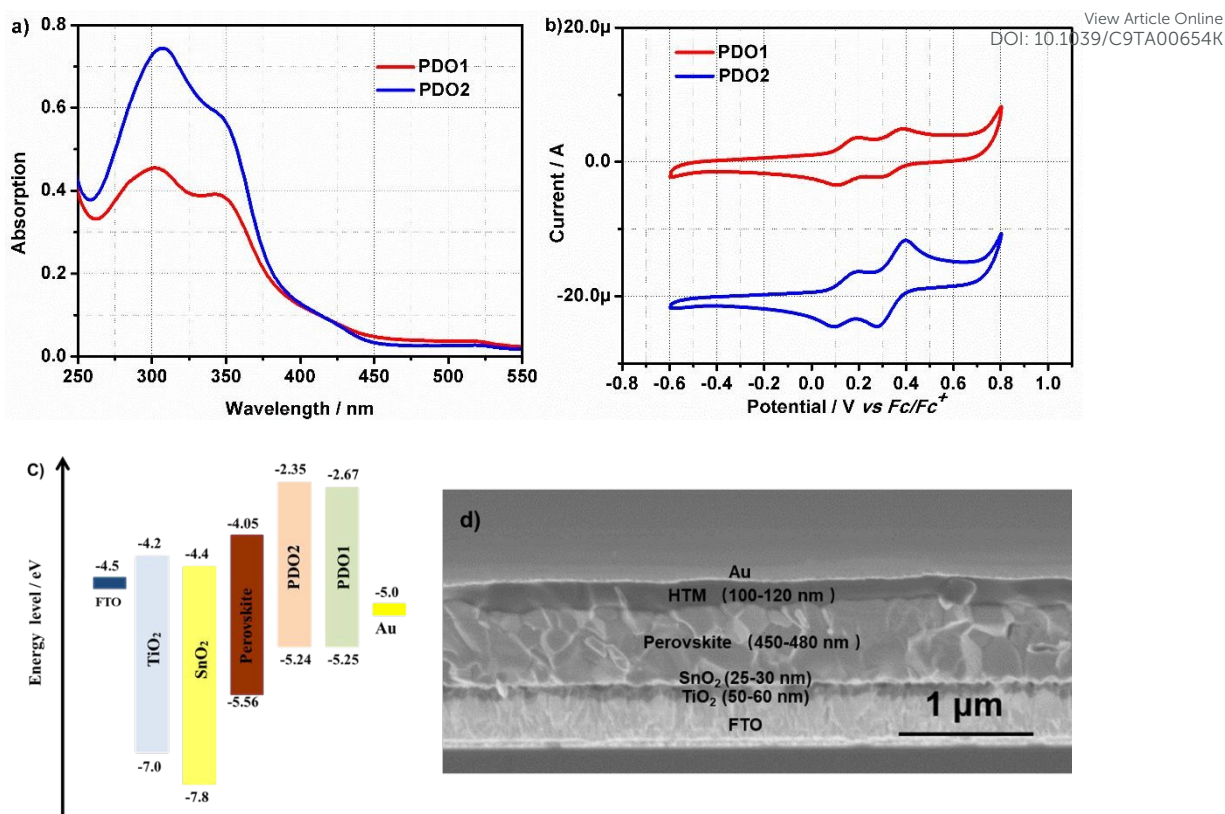


Figure 3 a) UV-vis absorption spectra of PDO1 and PDO2, b) CV of HTMs PDO1 and PDO2 in chloroform solution, c) Schematic energy level diagram of PSC, d) Cross-section SEM of PSC

To evaluate whether these two new HTMs possess appropriate energy levels for application in PSCs, UV-vis absorption and cyclic voltammetry (CV) were measured in chloroform solution. The test results are shown in Figure 3a and Figure 3b. The energy-levels of the main device components used in this study are illustrated in Figure 3c. The HOMO energy levels of PDO1 and PDO2 are calculated to be -5.25 and -5.24 eV vs vacuum, respectively, which are much more positive than the valence band (VB) of the mixed perovskite used here, suggesting hole extraction is favorable from energy level point.^{32, 33} Obviously, the almost invariable HOMO energy levels of PDO1 and PDO2 indicate the *N*-substitution has negligible influence on HOMO levels. Compared with HTM PTZ1 (-4.77 eV) with PTZ as core building block reported by Grisorio,¹⁰ the oxidation of sulfur atom to sulfuryl in our case renders more negative HOMO levels, which is particularly appropriate for application in PSCs. By combining the CV and the UV-vis absorption test data, the LUMO energy levels of PDO1 and PDO2 were roughly

estimated to be -2.67 and -2.35 eV vs vacuum, respectively, which are high enough for electron blocking.^{32,33}

Density functional theory (DFT) calculations were performed by using Gaussian program at the B3LYP/6-31G (+d) level to gain insight of the charge distribution of PDO1 and PDO2. The calculated results are shown in Figure 4. The optimized molecular structures are well consistent with crystal structures. From the results we can find that the *N*-substitution has nearly no effects on charge distribution, which agrees well with that from CV measurements. For PDO1 and PDO2, the HOMO delocalizes on the whole molecular backbone, while the LUMO levels shift to the PDO core unit. The overlaps between HOMO and LUMO suggest the existence of strong Coulomb interaction, which is beneficial for hole extraction and transport.¹⁰ The calculated hole reorganization energies of PDO1 and PDO2 are 172 and 126 meV, respectively. The smaller reorganization energy suggests that PDO2 may have a higher hole mobility than PDO1. The hole mobilities of HTM PDO1 and PDO2 were calculated to be 1.76×10^{-4} and $5.93 \times 10^{-4} \text{ cm}^2 \cdot \text{V}^{-1} \cdot \text{s}^{-1}$ (see Figure S8a), respectively, By using space-charge-limited current (SCLC) model.¹² The result is exactly consistent with the DFT calculation results.

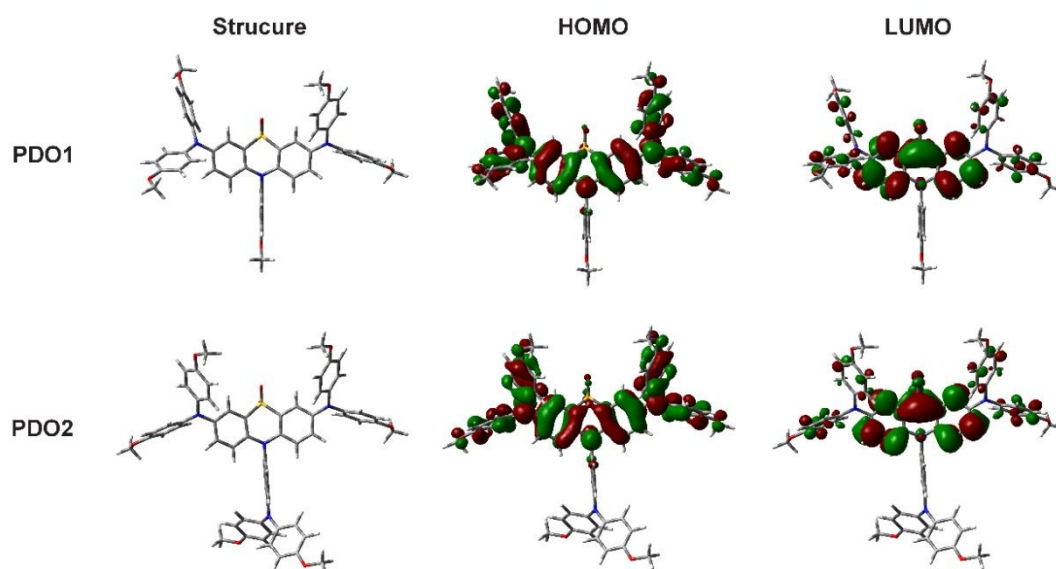


Figure 4 DFT calculation results of PDO1 and PDO2

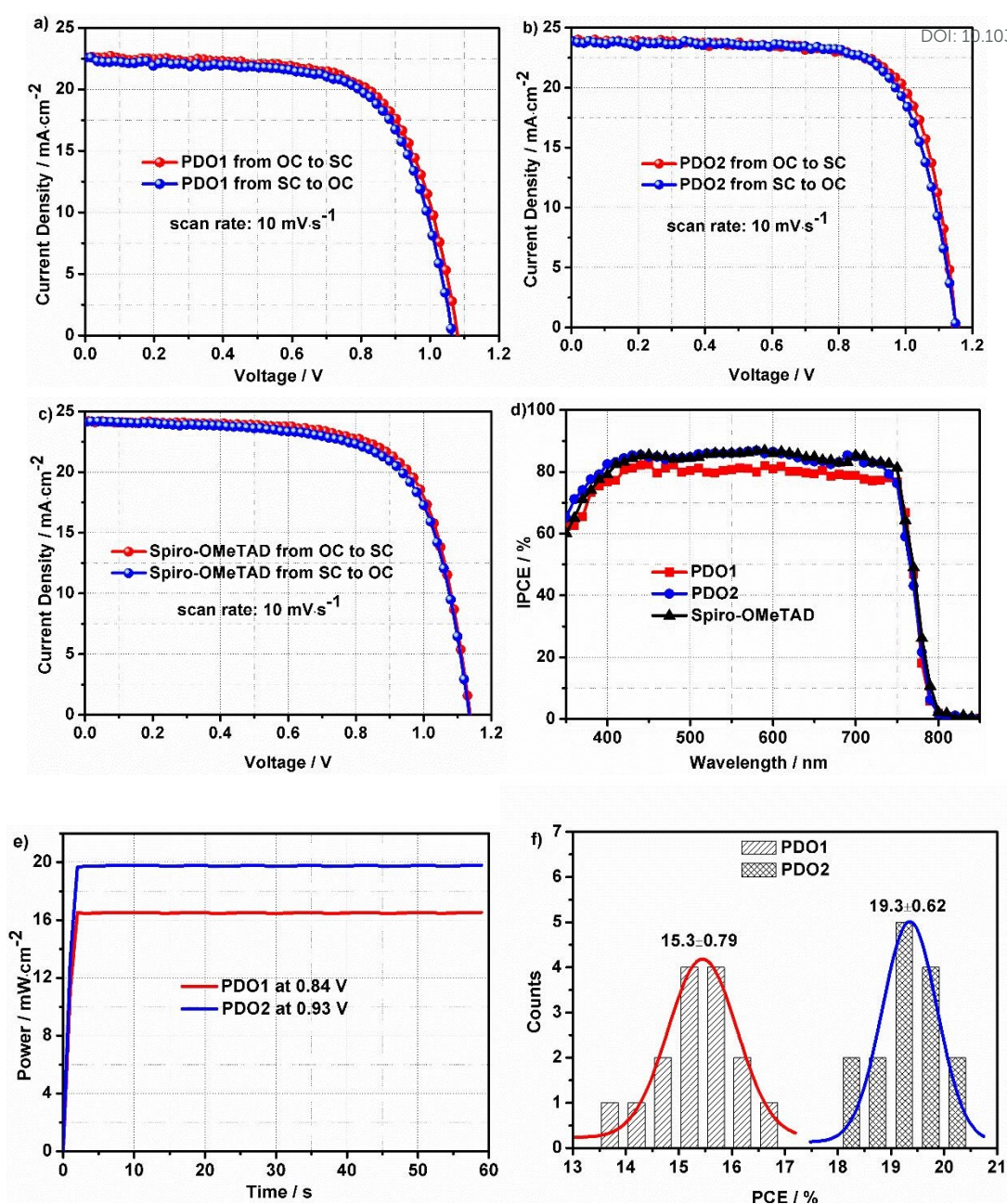


Figure 5 J - V characteristic curves of the PSCs containing a) PDO1, b) PDO2 and c) Spiro-OMeTAD as HTMs, d) IPCE spectra of PSCs containing PDO1, PDO2 and Spiro-OMeTAD as HTMs, e) steady-state power outputs at maximum point, f) statistics of PCE for PSCs containing PDO1 and PDO2 as HTMs

Table 1. The best photovoltaic performances of PSCs employing PTDO1, PTDO2 and Spiro-OMeTAD as HTMs

HTM	Scan direction	V_{oc} / V	$J_{sc} / \text{mA} \cdot \text{cm}^{-2}$	$FF / \%$	PCE / %	hysteresis index / %
PDO1	From OC to SC	1.08	22.6	68.3	16.7	0.025
	From SC to OC	1.07	22.7	67.7	16.4	
PDO2	From OC to SC	1.15	23.9	73.6	20.2	0.016
	From SC to OC	1.15	23.9	72.1	19.8	
Spiro-OMeTAD	From OC to SC	1.14	24.2	71.1	19.8	0.020
	From SC to OC	1.14	24.1	69.0	19.3	

Note: scan forward: from open circuit (OC) to short circuit (SC); scan backward: from short circuit (SC) to open circuit (OC).

We proceeded to test the synthesized HTMs in state-of-the-art planar PSCs with a detailed device structure of FTO/c-TiO₂/SnO₂/Perovskite/HTM/Au (see Figure 4d), and mixed halide perovskite (FAPbI₃)_{0.85}(MAPbBr₃)_{0.15} was employed as light-harvesting material. Figure 5a-5c display the current density-voltage (J - V) characteristic curves of the PSCs containing PDO1, PDO2 and Spiro-OMeTAD as HTMs. The devices were measured under a simulated AM 1.5 G (100 Mw.cm⁻²) sunlight with a slow scan rate of 10 mV · s⁻¹. The detailed parameters are showed in Table1. The PDO1- and PDO2-based devices show the best-performing PCE of 16.7% and 20.2%, respectively, especially the PDO2 even achieved higher champion PCE than reference HTM Spiro-OMeTAD (19.8%). From the IPCE spectra (Figure 5d), the estimated integrated

current densities are 22.0, 23.4 and 23.5 mA.cm⁻² for PDO1, PDO2 and Spiro-OMeTAD, respectively, which are agree well with the J_{sc} values acquired from the $J-V$ curves (error values lower than 5%). The stabilized power outputs at maximum point for PDO1- and PDO2-based are 16.4% and 19.5% (see Figure 5f), respectively, consisting with the $J-V$ measurements. The hysteresis index (HI) were calculated to be 0.025, 0.016 and 0.020 for PDO1-, PDO2- and Spiro-OMeTAD-based PSCs, respectively. The negligible hysteresis behavior indicates highly efficient charge carriers transport at the interfaces with the electron and hole-selective contacts. Compared with PDO1-based devices, the PSCs based on PDO2 exhibited higher open-circuit voltages (V_{oc}), short-circuit current densities (J_{sc}), and fill factors (FF). As is well known, the J_{sc} is closely related to light-harvesting efficiency, charge separation efficiency and charge collection efficiency. Considering the same fabrication process and components except HTM, the higher J_{sc} for PDO2-based PSCs should mainly result from higher hole extraction efficiency, which is confirmed by PL decay results. As shown in Figure S9, the steady-state and time-resolved PL decay measurements indicate the perovskite/PDO2 system showed much higher hole extraction efficiency and hole extraction rate than PDO1-based one, indicating hole transport in PDO2 based PSCs is more efficient. This is consistent with the higher PCE for PDO2 based device. The similar PL decay behavior for PDO2- and Spiro-OMeTAD-based system suggests the hole transport properties of PDO2 and Spiro-OMeTAD are comparable with each other. The higher IPCE values in entire response region for PDO2-based PSCs are also agreed perfectly with the $J-V$ and steady-state PL decay measurements discussed above. The improved FF can mainly be ascribed to the higher conductivity of PDO2-based hole transport layer (HTL) (see Figure S8b). To gain further explanations of higher V_{oc} for PDO2-based PSCs, the light intensity dependence of J_{sc} and V_{oc} were performed, as shown in Figure 6. It is worth noticing that PDO2-based PSCs exhibit stronger law dependence value ($\alpha = 0.905$) of the J_{sc} on light intensities, while weaker dependence of V_{oc} on light intensities ($1.23kT/q$). The results indicate the improved V_{oc} mainly

arises from highly restricted Shockley–Read–Hall (SRH) recombination during working process.³⁴ As shown in Figure 5f, PDO1- and PDO2-based PSCs also show excellent reproducibility with average PCEs of 15.3 ± 0.79 and 19.3 ± 0.62 , respectively, and the majority of devices obtained above-average PCEs. To better demonstrate the important effects of sulfuryl group, PTZ1 based PSCs were also evaluated for comparison. Expectedly, PDO1-based PSCs exhibit better photovoltaic performance (see Figure S10). The test results clearly show that except the peripheral groups adjustments, the oxidation sulfur atom to sulfone is also an effective molecular engineering mean to enhance the charge carrier mobility and their photovoltaic performance.

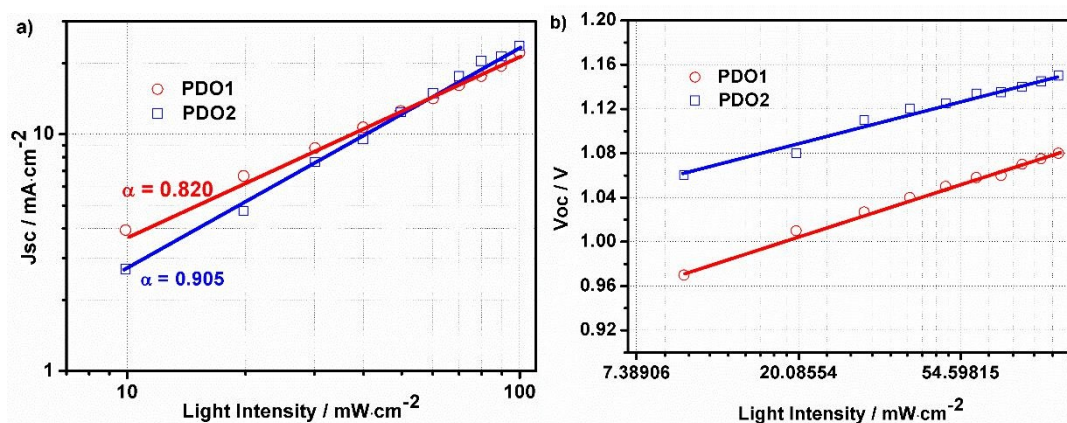
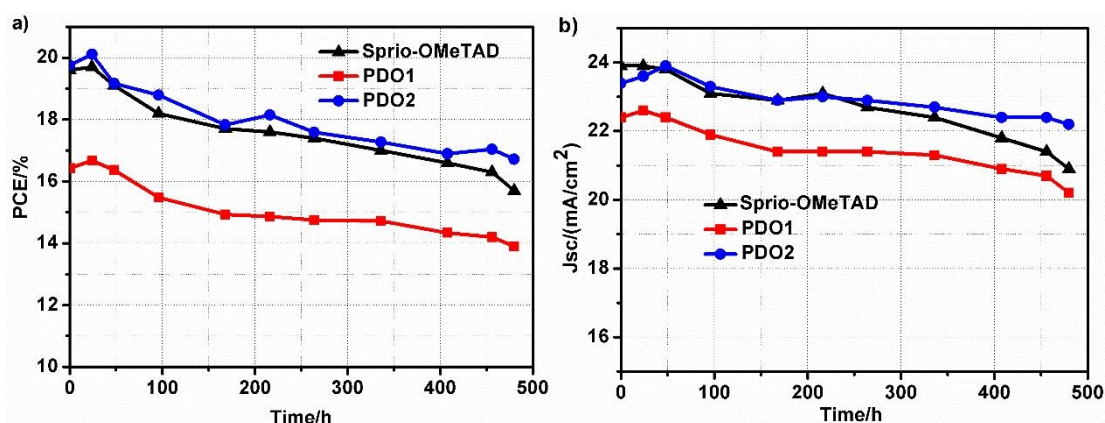


Figure 6 a) The dependence of J_{sc} on different light intensities, b) the dependence of V_{oc} on different light intensities



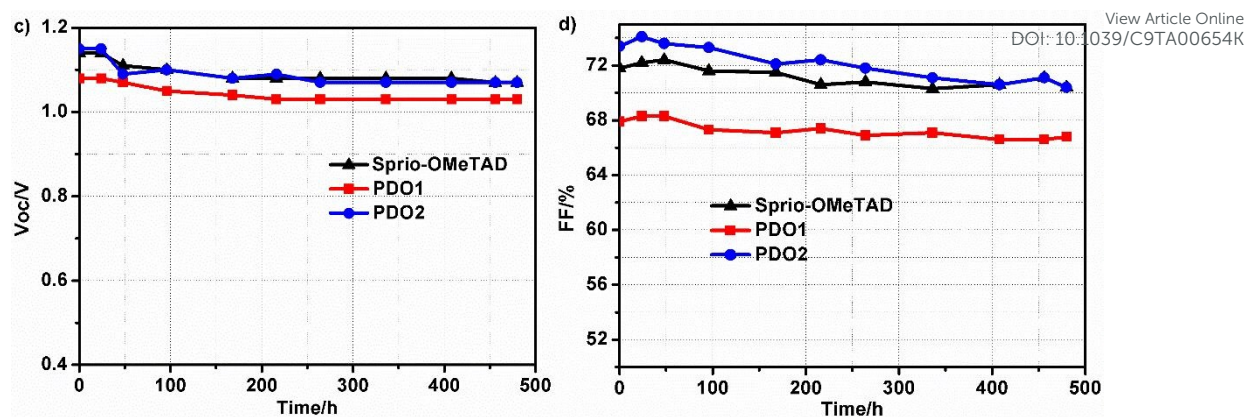


Figure 7 Aging test results a) PCE, b) J_{sc} , c) V_{oc} and d) FF of PSCs containing PDO1, PDO2 and Spiro-OMeTAD as HTMs

Figure 7a-7d shows the stability test results of the corresponding PSCs in air condition (relative humidity of 30-45%, room temperature) without encapsulation. The PDO1-, PDO2- and Spiro-OMeTAD based PSCs maintained 84.6%, 84.7% and 80.1% of the initial PCEs after 480 hours aging. The thermogravimetric analysis results (see Figure S11) show that PDO1 and PDO2 begin to decompose at 420 °C. Considering the good thermal stability of PDO1 and PDO2, the PCE decay might mainly cause by the dopants in HTL and the degradation of perovskite film.^{35,36} Therefore, our further research will focus on developing PDO core unit-based dopant-free HTMs.

In conclusion, we demonstrated that the oxidation of sulfur atom to sulfonyl and molecular engineering on *N*-substitution dramatically influenced the molecular configuration and photovoltaic performance of HTMs PDO1 and PDO2. Through the introduction of sulfonyl group on core building block, the electron density distribution, as well as HOMO levels, can be effectively adjusted. Importantly, PDO1 and PDO2 with the introduction of sulfonyl, possess particularly appropriate energy level alignment, excellent charge carrier mobility and the dramatically improved photovoltaic performance, in comparison with previously reported PTZ1. A PCE as high as 20.2% was achieved by PDO2-based PSC, which can be mainly attributed to the more planar geometry of PDO core unit and much stronger molecular stacking behavior. PDO2 is among the very few HTMs that can rival with Spiro-OMeTAD. This work reveals a great potential of the PDO building block for further development of

low-cost and highly-efficient HTMs for PSCs.

View Article Online
DOI: 10.1039/C9TA00654K

Acknowledgements

This work was financially supported by the Natural Science Foundation of Jiangsu province (BK20180867, BK20180869), National natural science foundation of China (Grants 21805114), the Jiangsu University Foundation (17JDG032, 17JDG031), High-tech Research Key laboratory of Zhenjiang (SS2018002), the high-performance computing platform of Jiangsu University, the Priority Academic Program Development of Jiangsu Higher Education Institutions

Supporting Information

The experimental details, characterization of HTMs, hole mobility and conductivity of HTMs, PL decay and thermogravimetric analysis results, supplied as Supporting Information.

Reference

1. A. Kojima, K. Teshima, Y. Shirai and T. Miyasaka, *J. Am. Chem. Soc.*, **2009**, *131*, 6050-6051.
2. N. J. Jeon, H. Na, E. H. Jung, T.-Y. Yang, Y. G. Lee, G. Kim, H.-W. Shin, S. Il Seok, J. Lee and J. Seo, *Nature Energy*, **2018**, *3*, 682-689.
3. N. J. Jeon, J. H. Noh, W. S. Yang, Y. C. Kim, S. Ryu, J. Seo and S. I. Seok, *Nature*, **2015**, *517*, 476-480.
4. D. Bi, W. Tress, M. I. Dar, P. Gao, J. Luo, C. Renevier, K. Schenk, A. Abate, F. Giordano, J.-P. C. Baena, J.-D. Decoppet, S. M. Zakeeruddin, M. K. Nazeeruddin, M. Grätzel and A. Hagfeldt, *Sci. Adv.*, **2016**, *2*, e1501170.
5. H. Zhou, Q. Chen, G. Li, S. Luo, T. B. Song, H. S. Duan, Z. Hong, J. You, Y. Liu and Y. Yang, *Science*, **2014**, *345*, 542-546.
6. M. L. Petrus, T. Bein, T. J. Dingemans and P. Docampo, *J. Mater. Chem. A*, **2015**, *3*, 12159-12162.
7. Michiel L. Petrus, A. Music, A. C. Closs, J. C. Bijleveld, M. T. Sirtl, Y. Hu, T. J. Dingemans, T. Bein and P. Docampo, *J. Mater. Chem. A*, **2017**, *5*, 25200-25210.

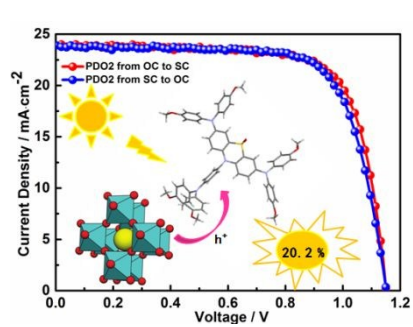
8. C. Chen, X. Ding, H. Li, M. Cheng, H. Li, L. Xu, F. Qiao and H. Li, *ACS Appl. Mater. Interfaces*, **2018**, *10*, 36608-36614.
9. C. Chen, H. Li, X. Ding, M. Cheng, H. Li, L. Xu, F. Qiao, H. Li and L. Sun, *ACS Appl. Mater. Interfaces*, **2018**, *10*, 38970-38977.
10. R. Grisorio, B. Roose, S. Colella, A. Listorti, G. P. Suranna and A. Abate, *ACS Energy Lett.*, **2017**, *2*, 1029-1034.
11. F. Zhang, S. Wang, H. Zhu, X. Liu, H. Liu, X. Li, Y. Xiao, S. M. Zakeeruddin and M. Grätzel, *ACS Energy Lett.*, **2018**, *3*, 1145-1152.
12. M. Cheng, Y. Li, M. Safdari, C. Chen, P. Liu, L. Kloo and L. Sun, *Adv. Energy Mater.*, **2017**, *7*, 1602556.
13. M. Cheng, B. Xu, C. Chen, X. Yang, F. Zhang, Q. Tan, Y. Hua, L. Kloo and L. Sun, *Adv. Energy Mater.*, **2015**, *5*, 1401720.
14. K. Gao, B. Xu, C. Hong, X. Shi, H. Liu, X. Li, L. Xie and A. K.-Y. Jen, *Adv. Energy Mater.*, **2018**, *8*, 1800809.
15. D. Vaitukaityte, Z. Wang, T. Malinauskas, A. Magomedov, G. Bubniene, V. Jankauskas, V. Getautis and H. J. Snaith, *Adv. Mater.*, **2018**, *30*, e1803735.
16. A. Molina-Ontoria, I. Zimmermann, I. Garcia-Benito, P. Gratia, C. Roldan-Carmona, S. Aghazada, M. Graetzel, M. K. Nazeeruddin and N. Martin, *Angew. Chem. Int. Ed.*, **2016**, *55*, 6270-6274.
17. K. Rakstys, M. Saliba, P. Gao, P. Gratia, E. Kamarauskas, S. Paek, V. Jankauskas and M. K. Nazeeruddin, *Angew. Chem. Int. Ed.*, **2016**, *55*, 7464-7468.
18. L. Calió, S. Kazim, M. Grätzel and S. Ahmad, *Angew. Chem. Int. Ed.*, **2016**, *55*, 14522-14545.
19. B. Xu, J. Zhang, Y. Hua, P. Liu, L. Wang, C. Ruan, Y. Li, G. Boschloo, E. M. J. Johansson, L. Kloo, A. Hagfeldt, A. K. Y. Jen and L. Sun, *Chem*, **2017**, *2*, 676-687.
20. M. Cheng, C. Chen, K. Aitola, F. Zhang, Y. Hua, G. Boschloo, L. Kloo and L. Sun, *Chem. Mater.*, **2016**, *28*, 8631-8639.
21. M. Cheng, C. Chen, X. Yang, J. Huang, F. Zhang, B. Xu and L. Sun, *Chem*.

- Mater.*, **2015**, *27*, 1808-1814.
22. C. Huang, W. Fu, C. Z. Li, Z. Zhang, W. Qiu, M. Shi, P. Heremans, A. K. Jen and H. Chen, *J. Am. Chem. Soc.*, **2016**, *138*, 2528-2531.
23. W. Ke, P. Priyanka, S. Vegiraju, C. C. Stoumpos, I. Spanopoulos, C. M. M. Soe, T. J. Marks, M. C. Chen and M. G. Kanatzidis, *J. Am. Chem. Soc.*, **2018**, *140*, 388-393.
24. B.-B. Cui, N. Yang, C. Shi, S. Yang, J.-Y. Shao, Y. Han, L. Zhang, Q. Zhang, Y.-W. Zhong and Q. Chen, *J. Mater. Chem. A*, **2018**, *6*, 10057-10063.
25. Y. Liu, Q. Chen, H.-S. Duan, H. Zhou, Y. Yang, H. Chen, S. Luo, T.-B. Song, L. Dou, Z. Hong and Y. Yang, *J. Mater. Chem. A*, **2015**, *3*, 11940-11947.
26. D. Bi, B. Xu, P. Gao, L. Sun, M. Grätzel and A. Hagfeldt, *Nano Energy*, **2016**, *23*, 138-144.
27. C. Chen, M. Cheng, P. Liu, J. Gao, L. Kloo and L. Sun, *Nano Energy*, **2016**, *23*, 40-49.
28. M. Cheng, K. Aitola, C. Chen, F. Zhang, P. Liu, K. Sveinbjörnsson, Y. Hua, L. Kloo, G. Boschloo and L. Sun, *Nano Energy*, **2016**, *30*, 387-397.
29. M. Wu, J. Li, R. Zhang, X. Tian, Z. Han, X. Lu, K. Guo, Z. Liu and Z. Wang, *Org. Lett.*, **2018**, *20*, 780-783.
30. H. Zhang, Y. Wu, W. Zhang, E. Li, C. Shen, H. Jiang, H. Tian and W. H. Zhu, *Chem. Sci.*, **2018**, *9*, 5919-5928.
31. Z. Li, Z. Zhu, C. C. Chueh, S. B. Jo, J. Luo, S. H. Jang and A. K. Jen, *J. Am. Chem. Soc.*, **2016**, *138*, 11833-11839.
32. N.-G. Park, *Mater. Today*, **2015**, *18*, 65-72.
33. H. S. Jung and N. G. Park, *Small*, **2015**, *11*, 10-25.
34. H. Zhang, J. Cheng, F. Lin, H. He, J. Mao, K. S. Wong, A. K. Jen and W. C. Choy, *ACS Nano*, **2016**, *10*, 1503-1511.
35. E. J. Juarez-Perez, M. R. Leyden, S. Wang, L. K. Ono, Z. Hawash and Y. Qi, *Chem. Mater.*, **2016**, *28*, 5702-5709.
36. S. Wang, Z. Huang, X. Wang, Y. Li, M. Gunther, S. Valenzuela, P. Parikh, A. Cabrerros, W. Xiong and Y. S. Meng, *J. Am. Chem. Soc.*, **2018**, *140*, 16720-

View Article Online
DOI: 10.1039/C9TA00654K

16730.

[View Article Online](#)
DOI: 10.1039/C9TA00654K



View Article Online
DOI: 10.1039/C9TA00654K

Two novel highly efficient and low-cost phenothiazine 5, 5-dioxide core building block based hole transport materials are reported, achieving power conversion efficiency as high as 20.2%.